CHEMISTRY
A EUROPEAN JOURNAL

FULL PAPER

DOI: 10.1002/chem.201301898

DFT Study on the Recovery of Hoveyda–Grubbs-Type Catalyst Precursors in Enyne and Diene Ring-Closing Metathesis

Francisco Núñez-Zarur, Xavier Solans-Monfort,* Roser Pleixats, Luis Rodríguez-Santiago, and Mariona Sodupe[a]

Abstract: DFT (B3LYP-D) calculations have been used to better understand the origin of the recovered Hoveyda–Grubbs derivative catalysts after ring-closing diene or enyne metathesis reactions. For that, we have considered the activation process of five different Hoveyda–Grubbs precursors in the reaction with models of usual diene and enyne reactants as well as the potential precursor regeneration through the release/return mechanism. The results show that, regardless of the nature of the initial precursor, the activation process needs to overcome relatively high energy barriers, which is in agreement with a relatively slow process. The precursor regeneration process is in all cases exergonic and it presents low energy barriers, particularly when compared to those of the activation process. This indicates that the precursor regeneration should always be feasible, unlike the moderate recoveries sometimes observed experimentally, which suggests that other competitive processes that hinder recovery should take place. Indeed, calculations presented in this work show that the reactions between the more abundant olefinic products and the active carbenes usually require lower energy barriers than those that regenerate the initial precatalyst, which could prevent precursor regeneration. On the other hand, varying the precursor concentration with time obtained from the computed energy barriers shows that, under the reaction conditions, the precursor activation is incomplete, thereby suggesting that the origin of the recovered catalyst probably arises from incomplete precursor activation.

Keywords: catalyst recovery · density functional calculations · metathesis · reaction mechanisms · ruthenium

Introduction

Since its accidental discovery about six decades ago, the olefin metathesis reaction has become one of the most important and effective procedures for the formation of carbon−carbon double bonds.[1–7] It refers to the exchange of carbon atoms (and their substituents) between two alkene molecules (Scheme 1) and depending on the nature of the reactants and/or the final products several subtypes of metathesis processes have been identified. Among them, the ring-closing metathesis of dienes (RCM) and enynes (RCEYM) involves the intramolecular rearrangement of reactants with two unsaturated fragments that lead to the formation of cyclic olefins and 1,3-conjugated cyclic dienes, respectively (Scheme 1). These reactions constitute powerful synthetic tools for the preparation of drugs, natural products, and a variety of other complex and useful organic molecules[8,9] and they are the target reactions of this work.

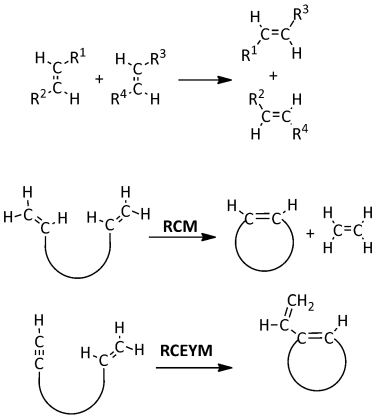

Scheme 1. Ring-closing metathesis of dienes (RCM) and enynes (RCEYM) involving the intramolecular rearrangement of reactants with two unsaturated fragments leading to the formation of cyclic olefins and 1,3-conjugated cyclic dienes.

Olefin metathesis only proceeds in the presence of an appropriate catalyst.[10–13] For this reason, catalyst development has attracted the attention of many research groups, thus

[a] Dr. F. Núñez-Zarur, Dr. X. Solans-Monfort, Prof. R. Pleixats, Dr. L. Rodríguez-Santiago, Prof. M. Sodupe
Departament de Química, Universitat Autònoma de Barcelona
Cerdanyola del Vallès 08290, Barcelona (Spain)
Fax: (+34) 935812920
E-mail: xavi@qf.uab.es

Supporting information for this article is available on the WWW under http://dx.doi.org/10.1002/chem.201301898. It contains the free energy profiles ($G+\Delta G_{solv}+D$) of all precatalyst activation processes, all precursor regeneration pathways, and for the nonproductive reactions; the optimized geometries of all stationary points associated with the precatalyst activation, with the precursor regeneration processes, and those of the nonproductive reactions; and the precatalyst concentration with time for the reaction of $\mathbf{3}_M$ with diene **c**.

leading to the synthesis of several very efficient, stable, and active catalysts.[3,8,14,15] Two main families of homogeneous catalysts can be distinguished: the Mo or W Schrock-type alkylidene complexes,[10,11] and the Ru-based Grubbs carbenes.[12,13] Ru-based catalysts are usually more stable and easier to handle and therefore they are the ones most commonly used in the laboratory nowadays. Figure 1 shows some of the most relevant Grubbs-type catalysts,[16–33] a particular case being complexes of the general formula shown in species **III** and **IV**, which are referred to as Hoveyda–Grubbs-type complexes.[29,31,33]

One important drawback of homogeneous catalytic reactions is the product–catalyst separation at the end of the catalytic cycle.[34,35] This means that even today most of the industrial reactions still rely on heterogeneous processes in which the reactants and the catalysts are in different phases.[14] In olefin metathesis catalyzed by Ru-based complexes, the product–catalyst separation is particularly relevant since an incomplete separation can lead to metal-contaminated products, which is an extremely important problem in the pharmaceutical industry owing to the relatively high toxicity of ruthenium.[36] Moreover, catalyst recyclability is also a key issue from an economical point of view because ruthenium is an expensive and scarce metal. Finally, it is also worth mentioning that the presence of metals after a metathesis reaction can promote undesired side reactions such as isomerization or degradation during workup.[37–39]

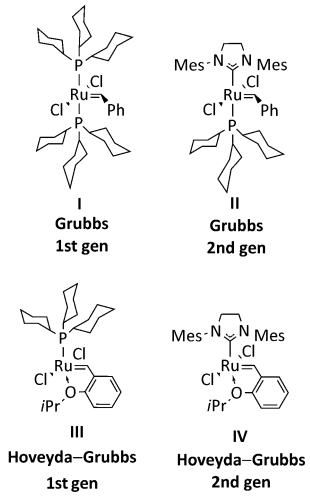

Figure 1. Some of the most relevant Grubbs-type catalysts.

In view of these disadvantages, several groups have synthesized heterogenized Mo-[34,35,40,41] and Ru-based[42–60] molecular complexes that can catalyze the olefin metathesis reaction, thereby combining the advantages of homogeneous catalysts (group tolerance, selectivity, and so on) with an easier product–catalyst separation.[34] For ruthenium carbenes, the supported catalysts have been prepared by diverse approaches that mainly differ in terms of the linking ligand and the nature of the support. The immobilization has been performed by means of one of the neutral two-electron donor ligands (the phosphine[42,56] or the N-heterocyclic carbene (NHC)[43,44,47,57–60]), through halogen exchange,[45,46,48,49] or through the alkylidene.[50–54] In particular, some of us prepared several organic–inorganic hybrid silica materials based on the second-generation Hoveyda–Grubbs catalyst **IV** (Figure 1).[52–54]

For those complexes anchored to the surface through the alkylidene fragment, it was initially proposed that the cata-

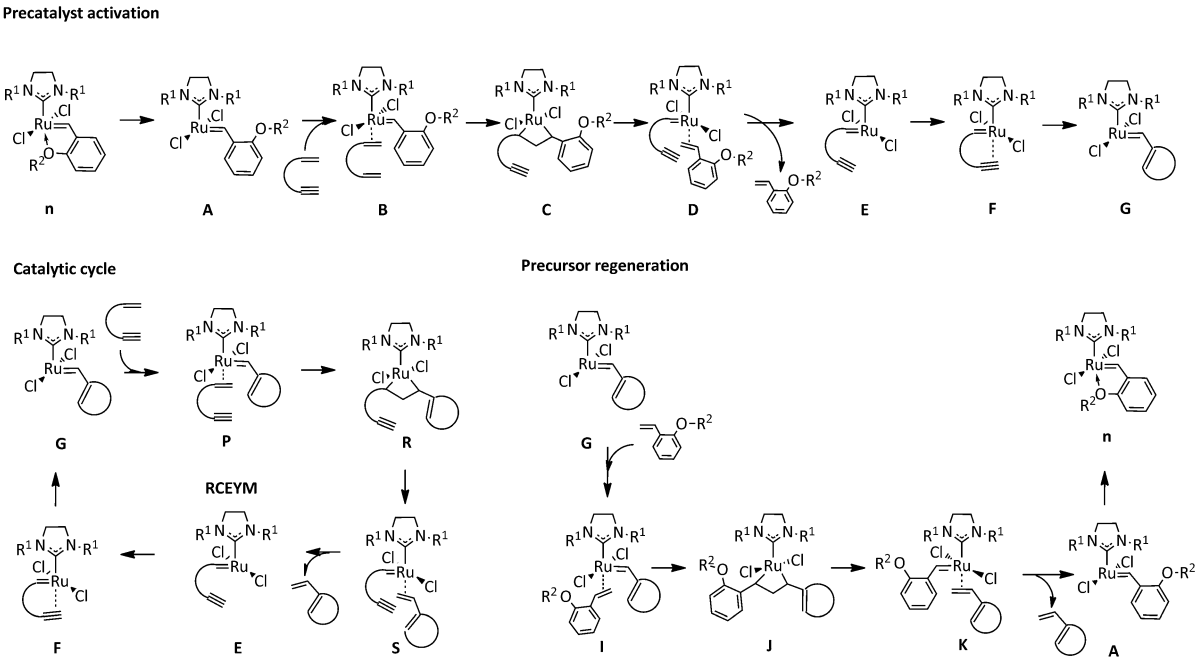

Scheme 2.

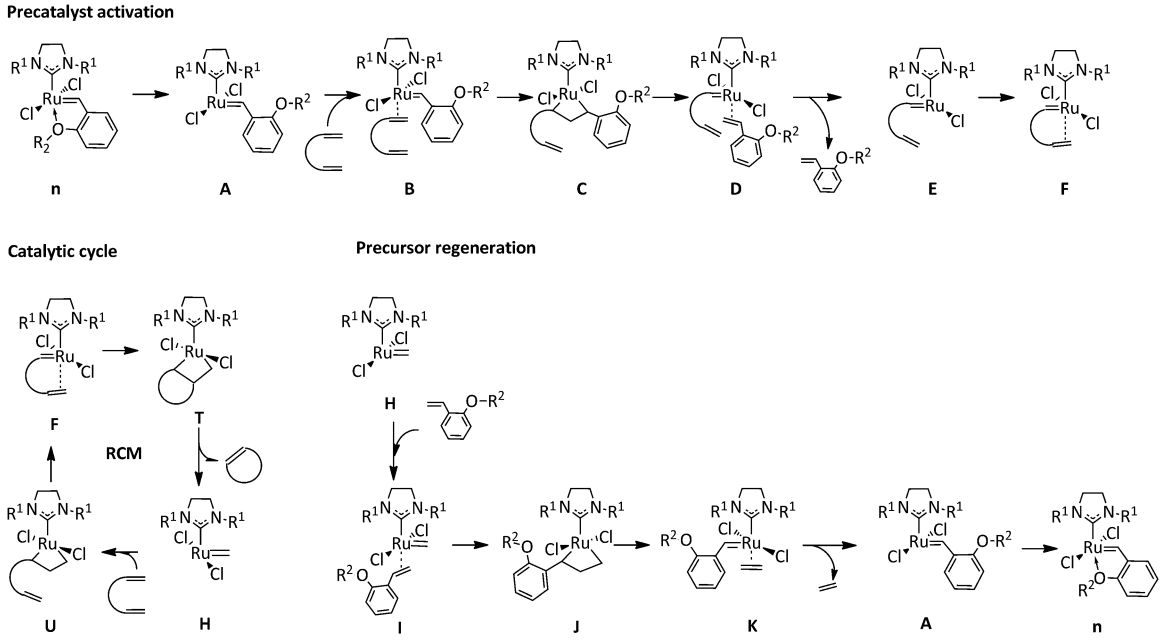

Scheme 3.

lyst recovery was associated with a release/return mechanism, also called a boomerang effect.[30,31,61] According to this mechanism, the active carbene species is released into the solution from the precatalyst during the activation process to carry out the productive metathesis reaction, and, once the reaction is completed, the precatalyst is regenerated by the reaction of intermediate carbene species with the benzylidene ligand (see Schemes 2 and 3). This concept was generalized to molecular Hoveyda–Grubbs complexes, which contain a bidentate benzylidene ether ligand, thereby suggesting that the release/return mechanism applies in homogeneous processes. In this way, Nolan and co-workers[24,27] and Grela and co-workers[62,63] (Figure 2), among others, have focused on the recovery properties of several Hoveyda–Grubbs-type catalysts in diene and enyne RCM reactions in solution. For these systems, the homogeneous catalyst recovery was from good to moderate and low at the end of the reaction depending on the structure of the precursor, the substrate involved in the reaction, and the percentage loading of the precatalyst.

More recently, Plenio and co-workers have shown by means of fluorescence spectroscopy and UV-visible experiments that the release/return mechanism does not contribute to the regeneration of several Hoveyda–Grubbs-type precursors to a significant extent,[64] thereby concluding that the boomerang effect does not apply under their reaction conditions. In view of these results, the proposed alternative explanation was that the amounts of recovered precursors might be due to the incomplete activation of the initial complex.

The olefin metathesis reaction catalyzed by either d^0 or Ru-based complexes has been the subject of a large number of computational works.[65–88] Nevertheless, to the best of our

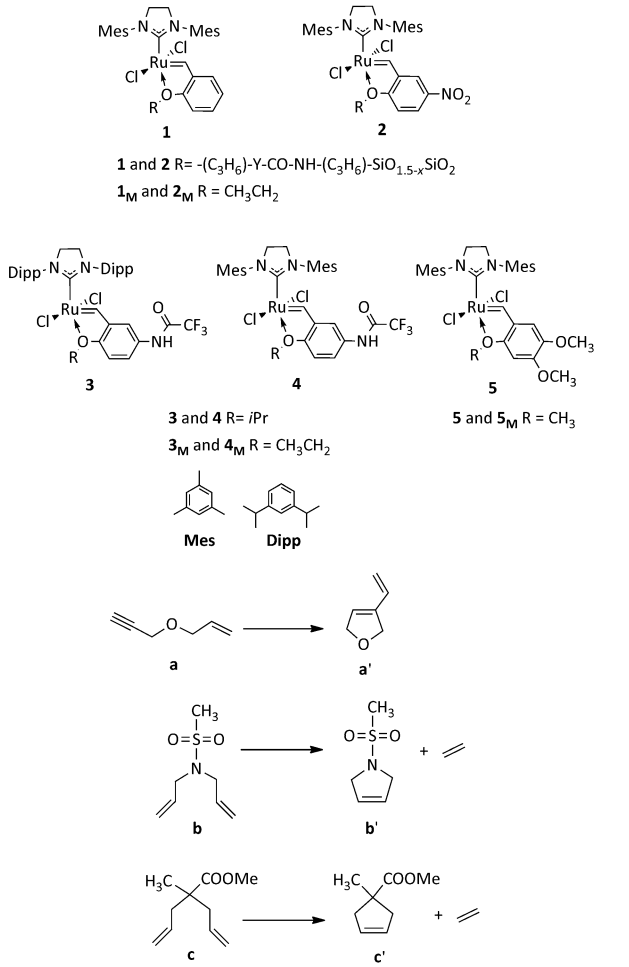

Figure 2. Models of the precursors ($\mathbf{1_M}$ to $\mathbf{5_M}$), substrates (**a**, **b**, and **c**) and products (**a′**, **b′**, and **c′**).

knowledge, theoretical studies focused on the viability of the boomerang effect have not been performed, and only a previous contribution from some of us has dealt with this topic indirectly.[84] In the current work, we study the precursor activation and their corresponding recovery process to discuss which of the two proposed origins of the recovered catalyst (release/return mechanism or incomplete precursor activation) is most likely according to DFT calculations. For this purpose, several enyne and diene RCM reactions with the Hoveyda–Grubbs-type precursors are studied (Figure 2).

Computational Details

Precursors and substrate molecules in this work were taken from the literature.[24,52,63] Figure 2 shows the models of the precursors ($\mathbf{1_M}$ to $\mathbf{5_M}$) and substrates (**a**, **b**, and **c**). The precursors are represented by the actual bulk except for the anchoring ether ligand/surface (**1** and **2**) and the isopropyl ether chelating groups (**3** and **4**), which have been replaced by ethyl ether groups. The only exception is complex **5**, which is represented with the actual bulk, and no simplifications were used. The reactants **a**, **b**, and **c** are models of the experimentally used substrates 1-allyloxy-1,1-diphenyl-2-propyne, *N*,*N*-diallyl-*p*-toluensulfonamide, and 2-allyl-2-methallylmalonate, respectively.

The methodology used in this work is similar to that used in our previous contributions on Ru-based olefin metathesis.[81–83,89] Full geometry optimizations were carried out in the gas phase using the B3LYP[90,91] density functional without any symmetry constraint and a basis set (**BS1**) that consisted of: 1) a 6-31G(d,p)[92,93] basis set for main-group elements, and 2) the quasirelativistic effective core pseudo-potentials (RECP) of the Stuttgart group[94,95] and the associated basis sets augmented with a polarization function for Ru.[96] Energetic refinement was made through single-point calculations at the **BS1**-optimized geometries using the same functional and **BS2**, a larger basis set that consists in the same representation for Ru and the 6-31++G(d,p) basis set for all other atoms.[97] The gas-phase thermal corrections were evaluated at 298.15 K and 1 atm with **BS1**. Solvent effects were taken into account by using the conductor-like polarizable continuum model (C-PCM).[98] The solvent was dichloromethane (CH_2Cl_2, $\varepsilon = 8.93$) and the used cavity was taken from the United Atom Topological Model on radii optimized at the HF/6-31G(d) level of theory (UAHF).[99] Dispersion contributions, which have been shown to be relevant in Ru-based olefin metathesis reactions,[70,78,100] were added a posteriori by using the methodology proposed by Grimme[101,102] as implemented in the Moldraw program.[103] The nature of all stationary points along the potential-energy surfaces was confirmed by the computation of the Hessian matrix. All calculations were performed using the Gaussian 03 program.[104]

In principle, the most realistic energies should be those based on the Gibbs energies in solution with gas-phase thermal corrections and the dispersion term $G_{gp}+\Delta G_{solv}+D$, as it includes all possible thermal and entropic effects from both solute and solvent. Nevertheless, models similar to the ones used here (in which solvent is not included explicitly) seem to overestimate both the entropic[105,106] and the dispersion contributions.[107–109] The former tends to destabilize all intermediates with respect to separated reactants, whereas the effect of the latter is the opposite (overstabilize the intermediates). In this context, the $E_{gp}+\Delta G_{solv}$ values (without the gas-phase entropic contribution and the dispersion forces) are also included in the text.

Results

Nomenclature: The nomenclature throughout the manuscript is constructed from 1) a capital letter (**A** to **F** or **G** for the activation and **G** or **H** to **n** for the precursor regeneration) that defines the nature of the minima as illustrated in Schemes 2 and 3; 2) a second capital letter that indicates if the intermediate belongs to a reaction in which the reactant of the catalytic process is an enyne (**E**) or a diene (**D**); and 3) an integer number with **M** as subscript that refers to the nature of the precursor ($\mathbf{1_M}$ to $\mathbf{5_M}$ according to Figure 2). The transition-state designation is constructed by adding "**TS**" before the capital letters that connect the two intermediates.

Generalities: Results are divided into three parts. First, we summarize the energetics of the activation process of precursors $\mathbf{1_M}$–$\mathbf{5_M}$ with all substrates **a**, **b**, and **c**. Secondly, we study the regeneration processes of the precursors through the boomerang effect, and finally, we compare the energetics of the regeneration process with those of the nonproductive metathesis processes that involves product olefins and the carbenes formed in the catalytic cycle. The considered reactions are summarized in Scheme 4. In this scheme, the black solid arrows describe the activation processes, and the gray dashed ones correspond to precursor regeneration.

In the case of the reactions with enyne **a**, two different mechanisms can be distinguished: the ene-then-yne pathway (first reaction of the alkene with the carbene) and the yne-then-ene pathway (first reaction of the alkyne with the carbene).[110–114] Therefore, depending on the mechanism applied during the activation process, two possible active species can be formed (**G** or methylidene). Nevertheless, Fogg and co-workers recently showed that in the absence of ethene in the reaction mixture, the methylidene species is not detected.[110] Moreover, our recent contribution on ring-closing enyne metathesis showed the larger stability of **G** (Scheme 2) relative to that of the methylidene, and that the latter can easily evolve into **G**.[83] These results suggest that in the absence of ethene, **G** would be the unique carbene in the reaction mixture and, therefore, in this manuscript, we only consider the activation process through the ene-then-yne pathway and, more importantly, the precursor regeneration from **G** (Scheme 2).

Activation mechanisms of precursors $\mathbf{1_M}$–$\mathbf{5_M}$: The activation process of Hoveyda–Grubbs-type precursors has already been studied in the literature, both experimentally[18,79,115–117] and theoretically.[79–82,84] Nowadays, it is accepted that among the three mechanisms initially proposed—associative,[117] dissociative,[20] and interchange[115]—the former can be excluded, and the applicability of the other two depends on the reacting alkene nature, alkene concentration, and size of the chelating ether group.[82,116] Our computational results showed that for reactants and catalysts similar to the ones studied here, the dissociative mechanism seems to be preferred, and therefore we only considered this pathway.[82] Nevertheless, we do not expect that the alkene coordination mechanism will be determinant because the energy differences between the dissociative and interchange mechanism in this part of the mechanism are small.[82]

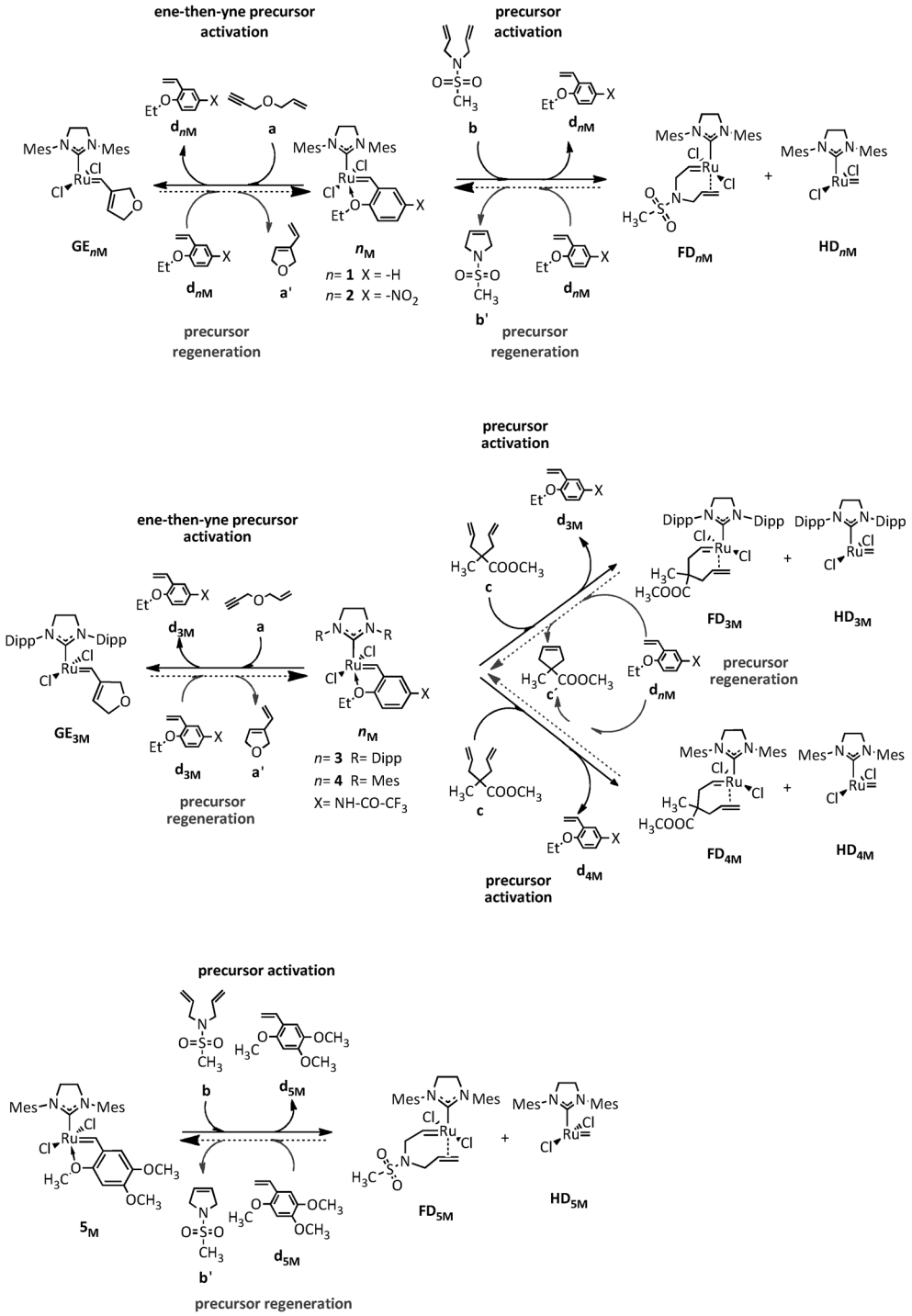

Scheme 4. Summary of the reactions under consideration in this paper.

Figures 3 and 4 show the Gibbs free-energy profile of the activation of precursors $\mathbf{3_M}$ by reaction with enyne **a** and diene **c**, respectively, as representative examples. The other Gibbs energy profiles are shown in Figures S1–S5 of the Supporting Information, and all stationary-point geometries (minimum and transition-state structures) are shown in Figures S6–S13 of the Supporting Information. Table 1 reports the highest transition structure of the precursor activation process for all considered systems as well as their Gibbs energy with respect to separated reactants. For all studied complexes $\mathbf{1_M}$–$\mathbf{5_M}$, the active carbene generation process shares the same five first elementary steps that were already described in our previous works:[81,82] chelating ether dissociation, alkene coordination, cycloaddition, cycloreversion, and Hoveyda–ligand decoordination. This leads to the generation of a new carbene that bears the reacting alkene mol-

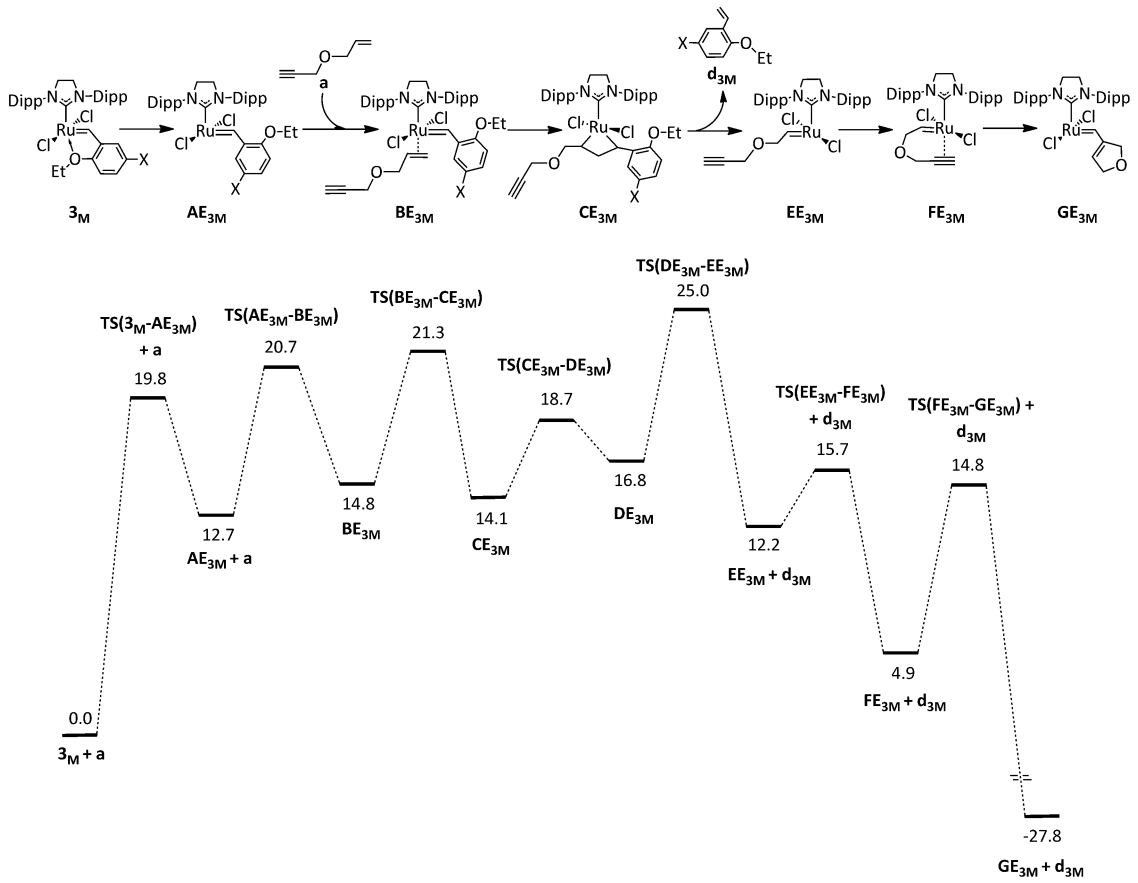

Figure 3. Gibbs free-energy profile ($G_{gp} + \Delta G_{solv} + D$, in kcal mol^{-1}) of the activation of precursor $\mathbf{3_M}$ by reaction with enyne **a**.

ecule (intermediate **E** in Schemes 2 and 3) and can easily further evolve into more stable species. For the particular case of the reactions that involve dienes, this implies the formation of a carbene in which the pendant alkene fragment of the reactant is coordinated to the metal center (**F** in Scheme 3, Figure 4, and Figures S2, S3, and S5 of the Supporting Information). In contrast, for the reactions that involve enynes, the formation of a more stable carbene implies the coordination of the alkyne and their subsequent rearrangement that leads to the conjugated carbene **G** (Scheme 2, Figure 3, and Figures S1 and S4 of the Supporting Information). The geometrical structures of all involved intermediates and transition structures (Figures S6–S13 in the Supporting Information) show similar features to those already reported[81,82] and therefore will not be discussed.

With regard to the energetics, the initial benzylidene dissociation leads to carbene **A**. This process is endergonic, and its reaction free energies range from 10.8 to 13.6 kcal mol^{-1} (between 10.0 and 11.5 kcal mol^{-1} in terms of $E_{gp}+\Delta G_{solv}$) depending on the nature of the precursor. The associated Gibbs energy barriers for this process lie between 18.7 and 21.8 kcal mol^{-1} (ranging from 15.5 and 18.5 kcal mol^{-1} in terms of $E_{gp}+\Delta G_{solv}$), which are relatively high, and although they are usually not associated with the highest free-energy transition structure, they are the highest barriers for an individual step in the whole activation process (see below). In the second step, the reacting diene or enyne coordinates to **A**, thus generating complex **B**. The reaction Gibbs energies of the reactant coordination range between −1.5 and +4.7 kcal mol^{-1}, and the associated Gibbs free energy barriers are always lower than 12.4 kcal mol^{-1} (they range between 2.7 and 12.4 kcal mol^{-1}). Overall, the coordination process, which implies the exchange of the fifth ligand (chelating ether group versus alkene), is in all cases endergonic by about 9.5 to 18.3 kcal mol^{-1} (between 12.1 and 22.4 kcal mol^{-1} in terms of $E_{gp}+\Delta G_{solv}$) and entails overcoming Gibbs energy barriers that are at least 18.7 kcal mol^{-1} above separated reactants (between 18.7 and 26.0 kcal mol^{-1}).

From the olefin complex **B**, the so-called Chauvin mechanism takes place (cycloaddition (**TS**(**B**–**C**)) and cycloreversion (**TS**(**C**–**D**)) steps).[118,119] Overall, the formation of the olefin complex **D** through this Chauvin mechanism is essentially isoergonic (ΔG varies from −1.1 to 6.3 kcal mol^{-1}) and implies very low Gibbs energy barriers that are always lower than 6.7 kcal mol^{-1} (9.0 kcal mol^{-1} in terms of $E_{gp}+\Delta G_{solv}$). This suggests that once the alkene molecule has been coordinated, which is an unfavorable and energetically demanding process, the cycloaddition and cycloreversion steps are really fast processes, which is in agreement with

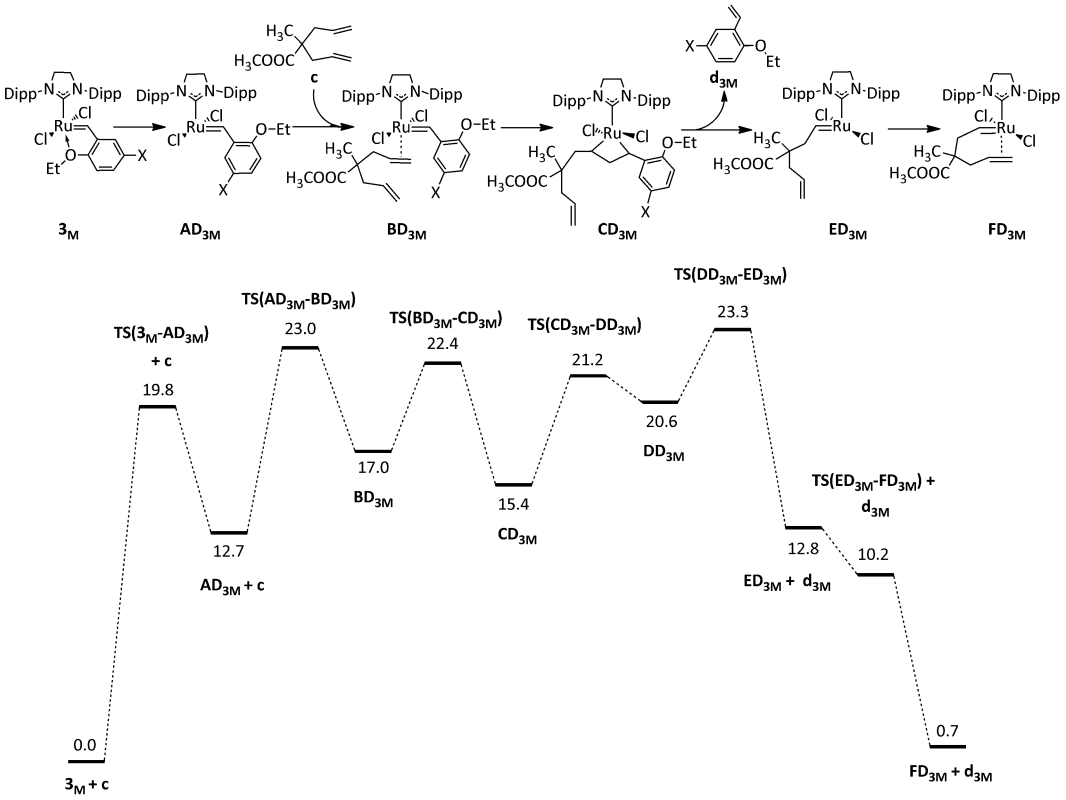

Figure 4. Gibbs free-energy profile ($G_{gp} + \Delta G_{solv} + D$, in kcal mol^{-1}) of the activation of precursor $\mathbf{3_M}$ by reaction with diene **c**.

Table 1. Reaction Gibbs energies (ΔG) for the precursor activation, the nature of the highest transition structure associated with this process, and Gibbs energy difference between the initial complex **n** (+the reacting olefin) and the highest transition structure of the precursor activation process ($\Delta G^{\neq}$). Both values based on $G_{gp}+\Delta G_{solv}+D$ and $E_{gp}+\Delta G_{solv}$ energies are reported [kcal mol^{-1}].

	$G_{gp}+\Delta G_{solv}+D$			$E_{gp}+\Delta G_{solv}$		
Reaction	ΔG	TS[a]	$\Delta G^{\neq}$	ΔE	TS	$\Delta E^{\neq}$
$\mathbf{1_M}$+**a**	−26.7	**TS(D–E)**	+25.4	−31.8	**TS(D–E)**	+19.8
$\mathbf{2_M}$+**a**	−27.8	**TS(D–E)**	+22.1	−34.0	**TS(D–E)**	+19.0
$\mathbf{1_M}$+**b**	−1.5	**TS(D–E)**	+25.2	+0.4	**TS(D–E)**	+24.9
$\mathbf{2_M}$+**b**	−2.6	**TS(D–E)**	+24.2	−1.8	**TS(D–E)**	+22.8
$\mathbf{3_M}$+**a**	−27.8	**TS(D–E)**	+25.0	−34.0	**TS(D–E)**	+21.8
$\mathbf{3_M}$+**c**	+0.7	**TS(D–E)**	+23.3	+2.8	**TS(D–E)**	+26.7
$\mathbf{4_M}$+**c**	+1.7	**TS(A–B)**	+26.0	+1.4	**TS(D–E)**	+23.7[b]
$\mathbf{5_M}$+**b**	−0.8	**TS(D–E)**	+28.0	+2.2	**TS(D–E)**	+26.8

[a] See Schemes 2 and 3 for structure definition. [b] The energy barrier associated with the coordination transition state **TS(A–B)** is 23.3 kcal mol^{-1}, and thus, highly competitive with **TS(D–E)**.

recent measurements on metallacyclobutane behavior.[120,121] The energetics of the benzylidene ligand release show that this process is exergonic but it needs to overcome Gibbs energy barriers that vary from 2.7 to 12.2 kcal mol^{-1} with respect to **D**. This means that this process is usually higher in energy than the steps associated with the Chauvin mechanism and thus it is usually associated with the highest free-energy transition structure of the whole activation process for the systems studied here.

The formation of the active species from carbene **E** is very exergonic with low energy barriers: between 0.8 and 3.6 kcal mol^{-1} for the intramolecular coordination and around 10 kcal mol^{-1} for the alkyne skeletal reorganization (for the case of enyne **a**). Overall, the highest Gibbs energy transition structures correspond to steps involved in the alkene metathesis process taking place once the reacting unsaturated molecule is coordinated to the metal center. This suggests that this cross-metathesis process is important in determining the feasibility of the precatalyst activation. The highest transition structures are located between 22.1 and 28.0 kcal mol^{-1} above the separated reactants (between 19.8 and 26.8 kcal mol^{-1} in terms of $E_{gp}+\Delta G_{solv}$), values that suggest that the activation can take place at room temperature but that this is not a fast process, especially when compared to the other processes studied in this work (see below).

Precursor regeneration of complexes $\mathbf{1_M}$–$\mathbf{5_M}$: The regeneration of precursors $\mathbf{1_M}$–$\mathbf{5_M}$ through the so-called boomerang effect would imply an olefin cross-metathesis reaction between a carbene of the catalytic cycle and the benzylidene ligand (the Hoveyda ligand) released in the activation process. In the case of the ring-closing enyne metathesis reaction, the most stable carbene of the catalytic cycle is **G** (Scheme 2), and the precursor regeneration has only been studied from this species. In contrast, for the ring-closing diene metathesis reaction, two different carbene complexes are involved in the catalytic cycle (**F** and **H**; Scheme 3). Pre-

cursor regeneration from **F** is the reverse reaction of the activation process, and thus it implies energy barriers that range from 22.6 to 28.8 kcal mol^{-1} (between 22.3 and 24.6 kcal mol^{-1} in terms of $E_{gp}+\Delta G_{solv}$). The regeneration from carbene **H** is the one discussed in this section, and it presents lower Gibbs energy barriers than the regeneration from **F** (see below). In any case, since **F** is the species that is lowest in energy of the catalytic cycle when the reaction involves diene molecules, $\mathbf{FD_{nM}+d_{nM}}$ (Scheme 4) is taken as origin of energies. Figures 5 and 6 show the Gibbs energy profiles for the precursor regeneration of complex $\mathbf{3_M}$ in the processes that involve enyne **a** and diene **c**, respectively. The free-energy profiles for all other complexes are shown in Figures S14–S18 of the Supporting Information.

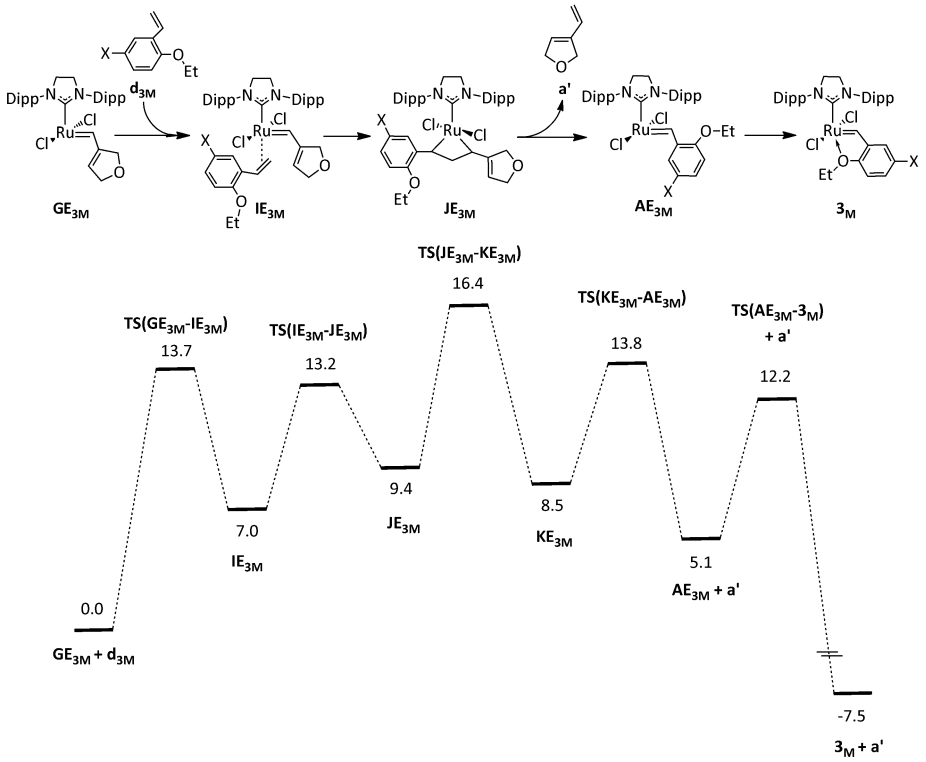

Figure 5. Gibbs energy profile ($G_{gp}+\Delta G_{solv}$ +D, in kcal mol^{-1}) for the $\mathbf{3_M}$ precursor regeneration in the process involving enyne **a**.

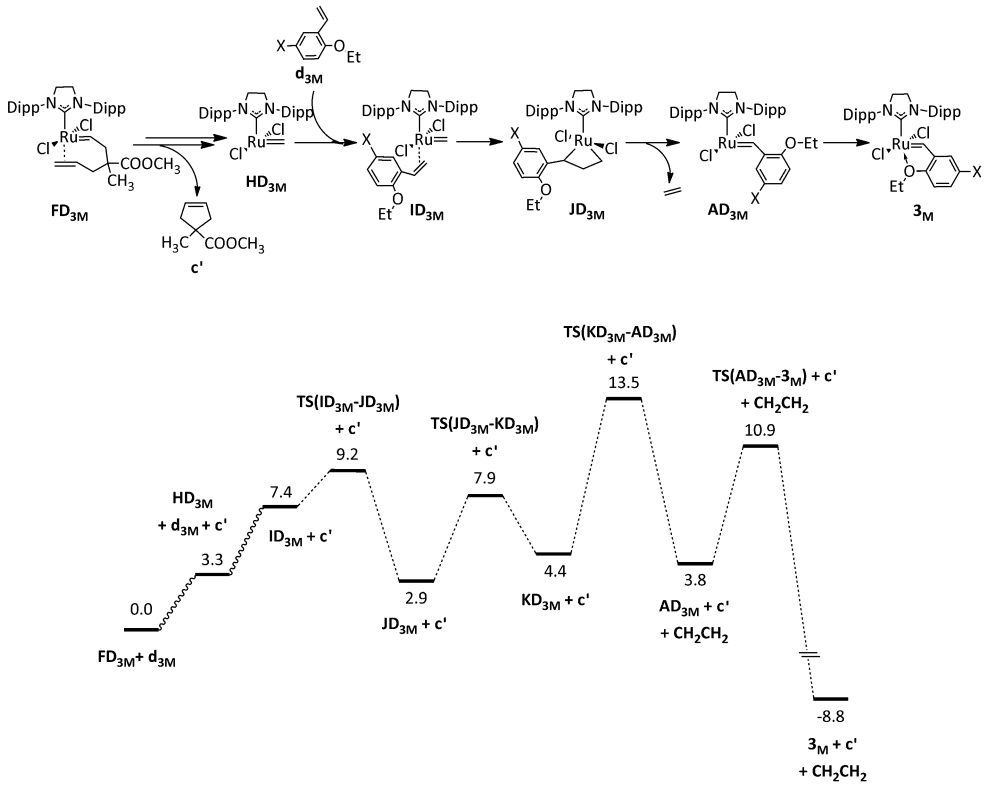

Figure 6. Gibbs energy profile ($G_{gp}+\Delta G_{solv}$ +D, in kcal mol^{-1}) for the $\mathbf{3_M}$ precursor regeneration in the process involving diene **c**.

All stationary-point geometries (minimum and transition-state structures) are shown in Figures S19–S26 of the Supporting Information. Table 2 summarizes the reaction Gibbs energies as well as the Gibbs energy difference between the most stable carbene of the catalytic cycle and the highest transition structure for all precursor regeneration processes considered here ($E_{gp}+\Delta G_{solv}$ values are added for comparison).

Table 2. Reaction Gibbs energies (ΔG) for the precursor regeneration, the nature of the highest transition structure associated with this process, and Gibbs energy difference between the most stable carbene of the catalytic cycle (+the released Hoveyda ligand) and the highest transition structure of the precursor regeneration process ($\Delta G^{\neq}$). Both values based on $G_{gp}+\Delta G_{solv}+D$ and $E_{gp}+\Delta G_{solv}$ energies are reported [kcal mol^{-1}].

	$G_{gp}+\Delta G_{solv}+D$				$E_{gp}+\Delta G_{solv}$	
Reaction	ΔG	TS[a]	$\Delta G^{\neq}$	ΔE	TS	$\Delta E^{\neq}$
GE$_{1M}$+d$_{1M}$	−8.7	**TS(K–A)**	+14.1	−6.5	**TS(J–K)**	+13.4
GE$_{2M}$+d$_{2M}$	−7.6	**TS(K–A)**	+15.5	−4.3	**TS(J–K)**	+14.4
FD$_{1M}$+d$_{1M}$	−7.8	**TS(K–A)**	+11.3	−2.8	**TS(A–1)**	+14.6
FD$_{2M}$+d$_{2M}$	−6.8	**TS(K–A)**	+14.7	−0.5	**TS(A–2)**	+15.0
GE$_{3M}$+d$_{3M}$	−7.5	**TS(J–K)**	+16.4	−4.2	**TS(J–K)**	+20.3
FD$_{3M}$+d$_{3M}$	−8.8	**TS(K–A)**	+13.5	−6.8	**TS(K–A)**	+10.7
FD$_{4M}$+d$_{4M}$	−8.6	**TS(K–A)**	+15.4	−2.5	**TS(K–A)**	+14.3
FD$_{5M}$+d$_{5M}$	−8.8	**TS(A–5)**	+12.2	−2.2	**TS(A–5)**	+16.1

[a] See Schemes 2, 3, and 4 for structure definitions.

We first focus on the regeneration process that involves an enyne as reactant. The cross-metathesis process involves five elementary steps: olefin coordination, cycloaddition, cycloreversion, releasing alkene (**a′**) decoordination, and coordination of the ether group of the Hoveyda ligand (Figure 5). Interestingly, regardless of the nature of the final complex, the precursor regeneration is always thermodynamically favorable, with the reaction Gibbs energies varying from −7.5 to −8.7 kcal mol^{-1} (between −4.2 and −6.5 kcal mol^{-1} in terms of $E_{gp}+\Delta G_{solv}$). Moreover, the computed Gibbs energy barriers are always relatively small, with the highest value for an individual step being 13.7 kcal mol^{-1} (15.6 kcal mol^{-1} in terms of $E_{gp}+\Delta G_{solv}$; Figure 5 and Figure S14 in the Supporting Information). This leads to an energy difference between the most stable carbene involved in the catalytic cycle and the highest transition structure ranging between 14.1 and 16.4 kcal mol^{-1} (between 13.4 and 20.3 kcal mol^{-1} in terms of $E_{gp}+\Delta G_{solv}$), which are values that suggest a feasible and relatively fast process at room temperature. That is, our calculations suggest that the so-called boomerang effect should be favorable both thermodynamically and kinetically in the RCEYM processes studied here.

The precursor regeneration process after a ring-closing diene metathesis implies the same five elementary steps: coordination, cycloaddition, cycloreversion, ethene decoordination, and coordination of the ether group of the Hoveyda ligand. The main difference to the process described for the catalytic RCEYM reaction is that the regeneration does not involve the most stable carbene **F** in solution, but rather the methylidene species (**H** in Scheme 3), which lies between +3.3 and +4.4 kcal mol^{-1} higher in Gibbs energy when the reacting species are **b** and **c**, respectively. This, however, has no significant effect on the overall precursor regeneration process; for all cases considered here, the reaction is also exergonic, with values varying between −6.8 and −8.8 kcal mol^{-1}, (between −0.5 and −6.8 kcal mol^{-1} in terms of $E_{gp}+\Delta G_{solv}$), and all computed energy barriers are relatively low, with the highest transition structures lying only between +11.3 and +15.4 kcal mol^{-1} higher in free energy than carbene **F** (between +10.7 and +16.1 kcal mol^{-1} in terms of $E_{gp}+\Delta G_{solv}$; Figure 6 and Figures S15, S16, and S18 in the Supporting Information). This suggests again that precursor regeneration should be feasible both from kinetic and thermodynamic points of view.

Nonproductive processes: We have also considered the reaction of **a′**,**b′** product olefins with the carbene **H** (for the diene; Scheme 3) and **G** (for the enyne; Scheme 2) through a cross-metathesis process (see Scheme 5). These are representative reactions for catalysts **1$_M$**, **2$_M$**, and **5$_M$** and can compete with the precursor regeneration because they share the same reacting carbene species. The free-energy profiles of these two reactions are shown in Figures S27 and S28 of the Supporting Information, whereas the stationary points involved in these processes are shown in Figures S29 and S30 in the Supporting Information. The mechanisms imply the same four steps as other cross-metathesis processes, and the reaction free energies are 0.0 and −4.4 kcal mol^{-1} for the

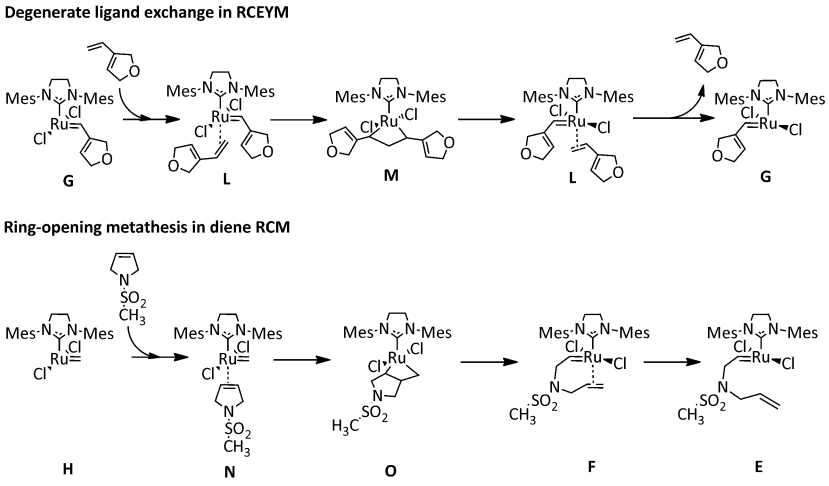

Scheme 5.

enyne (**a′**) and the diene (**b′**), respectively. Moreover, all individual steps show low energy barriers that range from 1.8 to 11.7 kcal mol^{-1}. Overall, the highest free-energy transition structures lie between 6.0 and 11.7 kcal mol^{-1} (between 4.3 and 9.3 kcal mol^{-1} in terms of $E_{gp}+\Delta G_{solv}$) above the separated reactants (Table 3). It is worth noting that these values

Table 3. Reaction Gibbs energies (ΔG) for the enyne and diene nonproductive processes, the nature of the highest transition structure associated with these processes, and the Gibbs energy difference between the system "active carbene + product olefin" and the highest transition structure of the nonproductive process ($\Delta G^{\neq}$).[a] Both values based on $G_{gp}+\Delta G_{solv}+D$ and $E_{gp}+\Delta G_{solv}$ energies are reported [kcal mol^{-1}].

	$G_{gp}+\Delta G_{solv}+D$			$E_{gp}+\Delta G_{solv}$		
Reaction	ΔG	TS	$\Delta G^{\neq}$	ΔE	TS	$\Delta E^{\neq}$
G+a′	0.0	**TS(G–L)**	+11.7	0.0	**TS(L–M)**	+9.3
H+b′	−4.4	**TS(N–O)**	+6.0	−6.3	**TS(O–F)**	+4.3

[a] See Scheme 5 for structure definitions.

are similar but lower than those computed for the precursor regeneration (compare Tables 2 and 3), and thus this seems to suggest that **G** and **H** carbenes, when available in the reaction mixture, would preferentially react with olefins **a′**, **b′** than with the benzylidene released one. Moreover, since **a′** and **b′** are expected to be more abundant than styrene $\mathbf{d_{nM}}$ (the latter is only present in catalytic concentrations), it is likely that the nonproductive processes could be predominant and thus prevent the precursor regeneration.

Discussion

The main goal of this work is to analyze whether the so-called boomerang effect could be operative in the recovery of several Hoveyda–Grubbs-type precursors in typical diene and enyne RCM reactions. The experimental data reported in Refs. [24], [52], and [63] show that the catalyst recovery of precursors **1**–**5** is not quantitative, although for some systems, the amounts of recovered precursor are significant. The calculations carried out here (Figures 5 and 6, and Figures S14–S18 in the Supporting Information) predict that the precursor regeneration from the active species is thermodynamically favored independently of the nature of the active carbene and olefin (Hoveyda ligand). The reaction free energies of precursor regeneration range from −8.8 to −6.8 kcal mol^{-1} and are therefore sufficiently favorable to act as driving forces. Moreover, all free-energy barriers are reasonably low, which are indicative of relatively fast processes. This might seem contradictory to the sometimes low to medium recoveries reported in the literature, but it is also worth pointing out that they are in line with 1) the fact that one usual synthetic route for the formation of Hoveyda–Grubbs-type complexes is the olefin cross-metathesis reaction between a phosphine-containing Ru-based precursor and the Hoveyda ligand (*o*-isopropoxystyrene) in stoichiometric quantities (Scheme 6)[30,33] and 2) the observation of small crossovers observed by Kingsbury and Hoveyda.[61]

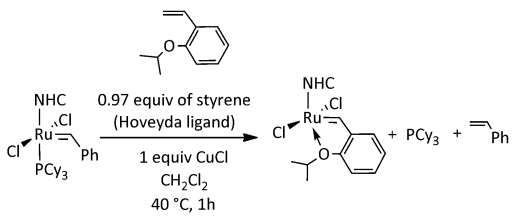

Scheme 6. A common synthetic route to the formation of Hoveyda–Grubbs-type complexes: The olefin cross-metathesis reaction between a phosphine-containing Ru-based precursor and the Hoveyda ligand in stoichiometric quantities.

Overall, the discrepancy between the experiments and the calculations seems to indicate that, although being favorable, the precursor regeneration does not take place—at least quantitatively—after the catalytic cycle. This could be due to the fact that the carbene species present in the reaction mixture are involved in other processes or deactivate. In particular, we have shown that the reaction with the more abundant product olefin implies similar to lower energetics than the precursor regeneration process, and thus this could be one of the factors that prevents the reaction with the released Hoveyda ligand.

Alternatively, it has been proposed that the amount of precursor obtained at the end of the catalytic cycle depends on the amounts of nonactivated initial complex.[64] In this way, a more difficult activation process would lead to an incomplete activation and, hence, just a fraction of the activated catalyst would then carry out the catalytic cycle. Within this idea, the harder the precursor activation is, the larger the amount of precursor obtained at the end of the catalytic process will be. Calculations carried out here predict that the activation processes are not thermodynamically disfavored (ΔG ranges from 1.7 to −27.8 kcal mol^{-1}), but the free-energy barriers involved are significantly higher ($\Delta G^{\neq}$ ranges from 22.1 to 28.0 kcal mol^{-1}) than those of the catalytic cycle,[77,78] those of the precursor regeneration ($\Delta G^{\neq} <$ 16.0 kcal mol^{-1}), and those of the other side reaction processes.

Interestingly, if one uses the energy barriers obtained in the present work to evaluate the precursor concentration with time,[122] it can be observed that no complete consumption of the initial precursor is achieved when considering the reaction conditions of Refs. [24], [52], and [63]. Kinetic constants are very sensitive to the energy barriers, and thus the evolution over time of the precursor concentration (Figure S31 of the Supporting Information for a selected example) has to be approached with care. Nevertheless, the calculations reported here go in the same direction as the experiments of Plenio and co-workers.[64] The usual reaction times employed in experiments seem not to be large enough to fully activate the original precursor, and thus the final amount of catalyst could be due to the nonactivated complex.

Conclusion

The DFT (B3LYP-D) calculations performed here on the activation process of several Hoveyda–Grubbs derivative precursors through the reaction of selected diene and enyne reactants (1-allyloxy-1,1-diphenyl-2-propyne, *N*,*N*-diallyl-*p*-toluensulfonamide, and dimethyl 2-allyl-2-methallylmalonate) as well as on the corresponding potential precursor regeneration after the catalytic cycle show that: 1) regardless of the nature of the Hoveyda–Grubbs precursor, the activation process presents relatively high energy barriers between +22.1 and +28.0 kcal mol^{-1}, which are consistent with a relatively slow process that takes place at room temperature, and 2) the precursor regeneration is always thermodynamically favorable (ΔG ranges from −8.8 to −6.8 kcal mol^{-1}) and kinetically easy ($\Delta G^{\neq}$ varies from +11.3 to +16.4 kcal mol^{-1}), thereby suggesting a feasible and fast process at room temperature. This seems to be inconsistent with an incomplete precatalyst recovery, which suggests that other competitive processes that hinder precursor regeneration might take place. In particular, the computed energetics of the processes associated with the reaction of the active carbenes with the more abundant product olefins ($\Delta G^{\neq}$ is between 6.0 and 11.7 kcal mol^{-1}) show that these processes require somewhat lower energy barriers than those of the precursor regeneration process. Consequently, these reactions as well as other similar ones could prevent the reaction between the initially released Hoveyda ligand and the carbenes involved in the catalytic cycle. More interestingly, the variation of the precursor concentration with time derived from present calculations suggests that—under normal reaction conditions—precursor activation is incomplete, and thus the experimentally recovered precatalyst amounts could likely be due to this incomplete activation, which is in agreement with the recent experiments of Plenio and coworkers.[64]

Acknowledgements

We acknowledge financial support from MICINN (CTQ2009-07881/BQU, CTQ2011-24847/BQU), Consolider Ingenio 2010 (project CSD2007-00006), and the Generalitat de Catalunya (SGR2009-638 and SGR2009-01441). F.N.Z wishes to thank the Universitat Autònoma de Barcelona for his PhD PIF scholarship. M.S. gratefully acknowledges support through the 2011 ICREA Academia award.

[1] N. Calderon, H. Y. Chen, K. W. Scott, *Tetrahedron Lett.* **1967**, *8*, 3327–3329.
[2] K. J. Ivin, J. C. Mol, *Olefin Metathesis and Metathesis Polymerization*, 2nd ed., Academic Press, San Diego, **1997**.
[3] K. J. Ivin, *J. Mol. Catal. A* **1998**, *133*, 1–16.
[4] A. H. Hoveyda, A. R. Zhugralin, *Nature* **2007**, *450*, 243–251.
[5] R. L. Banks, G. C. Bailey, *Ind. Eng. Chem. Prod. Res. Dev.* **1964**, *3*, 170–173.
[6] *Handbook of Metathesis, Vol. 1–3*, 1 st ed. (Ed.: R. H. Grubbs), Wiley-VCH, Weinheim, **2003**.
[7] R. H. Grubbs, *Tetrahedron* **2004**, *60*, 7117–7140.
[8] K. C. Nicolaou, P. G. Bulger, D. Sarlah, *Angew. Chem.* **2005**, *117*, 4564–4601; *Angew. Chem. Int. Ed.* **2005**, *44*, 4490–4527.
[9] M. Mori, *Adv. Synth. Catal.* **2007**, *349*, 121–135.
[10] R. R. Schrock, *Angew. Chem.* **2006**, *118*, 3832–3844; *Angew. Chem. Int. Ed.* **2006**, *45*, 3748–3759.
[11] R. R. Schrock, *Chem. Rev.* **2009**, *109*, 3211–3226.
[12] R. H. Grubbs, *Angew. Chem.* **2006**, *118*, 3845–3850; *Angew. Chem. Int. Ed.* **2006**, *45*, 3760–3765.
[13] G. C. Vougioukalakis, R. H. Grubbs, *Chem. Rev.* **2010**, *110*, 1746–1787.
[14] J. C. Mol, *J. Mol. Catal. A* **2004**, *213*, 39–45.
[15] C. Samojłowicz, M. Bieniek, K. Grela, *Chem. Rev.* **2009**, *109*, 3708–3742.
[16] S. T. Nguyen, R. H. Grubbs, J. W. Ziller, *J. Am. Chem. Soc.* **1993**, *115*, 9858–9859.
[17] S. T. Nguyen, L. K. Johnson, R. H. Grubbs, J. W. Ziller, *J. Am. Chem. Soc.* **1992**, *114*, 3974–3975.
[18] M. S. Sanford, J. A. Love, R. H. Grubbs, *J. Am. Chem. Soc.* **2001**, *123*, 6543–6554.
[19] M. S. Sanford, M. Ulman, R. H. Grubbs, *J. Am. Chem. Soc.* **2001**, *123*, 749–750.
[20] J. A. Love, J. P. Morgan, T. M. Trnka, R. H. Grubbs, *Angew. Chem.* **2002**, *114*, 4207–4209; *Angew. Chem. Int. Ed.* **2002**, *41*, 4035–4037.
[21] J. A. Love, M. S. Sanford, M. W. Day, R. H. Grubbs, *J. Am. Chem. Soc.* **2003**, *125*, 10103–10109.
[22] K. Endo, R. H. Grubbs, *J. Am. Chem. Soc.* **2011**, *133*, 8525–8527.
[23] B. K. Keitz, K. Endo, P. R. Patel, M. B. Herbert, R. H. Grubbs, *J. Am. Chem. Soc.* **2012**, *134*, 693–699.
[24] H. Clavier, F. Caijo, E. Borre, D. Rix, F. Boeda, S. P. Nolan, M. Mauduit, *Eur. J. Org. Chem.* **2009**, 4254–4265.
[25] A. Fürstner, O. R. Thiel, L. Ackermann, H. J. Schanz, S. P. Nolan, *J. Org. Chem.* **2000**, *65*, 2204–2207.
[26] J. K. Huang, E. D. Stevens, S. P. Nolan, J. L. Petersen, *J. Am. Chem. Soc.* **1999**, *121*, 2674–2678.
[27] D. Rix, F. Caijo, I. Laurent, F. Boeda, H. Clavier, S. P. Nolan, M. Mauduit, *J. Org. Chem.* **2008**, *73*, 4225–4228.
[28] K. Grela, S. Harutyunyan, A. Michrowska, *Angew. Chem.* **2002**, *114*, 4210–4212; *Angew. Chem. Int. Ed.* **2002**, *41*, 4038–4040.
[29] A. Michrowska, R. Bujok, S. Harutyunyan, V. Sashuk, G. Dolgonos, K. Grela, *J. Am. Chem. Soc.* **2004**, *126*, 9318–9325.
[30] S. B. Garber, J. S. Kingsbury, B. L. Gray, A. H. Hoveyda, *J. Am. Chem. Soc.* **2000**, *122*, 8168–8179.
[31] J. S. Kingsbury, J. P. A. Harrity, P. J. Bonitatebus, A. H. Hoveyda, *J. Am. Chem. Soc.* **1999**, *121*, 791–799.
[32] J. J. Van Veldhuizen, S. B. Garber, J. S. Kingsbury, A. H. Hoveyda, *J. Am. Chem. Soc.* **2002**, *124*, 4954–4955.
[33] S. Gessler, S. Randl, S. Blechert, *Tetrahedron Lett.* **2000**, *41*, 9973–9976.
[34] C. Copéret, J. M. Basset, *Adv. Synth. Catal.* **2007**, *349*, 78–92.
[35] C. Copéret, M. Chabanas, R. P. Saint-Arroman, J. M. Basset, *Angew. Chem.* **2003**, *115*, 164–191; *Angew. Chem. Int. Ed.* **2003**, *42*, 156–181.
[36] N. G. Anderson, *Practical Process Research and Development: A guide for Organic Chemists*, 2nd. ed., Academic Press, San Diego, **2000**.
[37] H. D. Maynard, R. H. Grubbs, *Tetrahedron Lett.* **1999**, *40*, 4137–4140.
[38] N. K. Yee, V. Farina, I. N. Houpis, N. Haddad, R. P. Frutos, F. Gallou, X. J. Wang, X. D. Wei, R. D. Simpson, X. W. Feng, V. Fuchs, Y. B. Xu, J. Tan, L. Zhang, J. H. Xu, L. L. Smith-Keenan, J. Vitous, M. D. Ridges, E. M. Spinelli, M. Johnson, K. Donsbach, T. Nicola, M. Brenner, E. Winter, P. Kreye, W. Samstag, *J. Org. Chem.* **2006**, *71*, 7133–7145.
[39] H. Clavier, K. Grela, A. Kirschning, M. Mauduit, S. P. Nolan, *Angew. Chem.* **2007**, *119*, 6906–6922; *Angew. Chem. Int. Ed.* **2007**, *46*, 6786–6801.
[40] F. Blanc, R. Berthoud, A. Salameh, J. M. Basset, C. Copéret, R. Singh, R. R. Schrock, *J. Am. Chem. Soc.* **2007**, *129*, 8434–8435.

[41] F. Blanc, C. Copéret, J. Thivolle-Cazat, J. M. Basset, A. Lesage, L. Emsley, A. Sinha, R. R. Schrock, *Angew. Chem.* **2006**, *118*, 1238–1242; *Angew. Chem. Int. Ed.* **2006**, *45*, 1216–1220.
[42] S. T. Nguyen, R. H. Grubbs, *J. Organomet. Chem.* **1995**, *497*, 195–200.
[43] S. C. Schürer, S. Gessler, N. Buschmann, S. Blechert, *Angew. Chem.* **2000**, *112*, 4062–4065; *Angew. Chem. Int. Ed.* **2000**, *39*, 3898–3901.
[44] M. Süßner, H. Plenio, *Angew. Chem.* **2005**, *117*, 7045–7048; *Angew. Chem. Int. Ed.* **2005**, *44*, 6885–6888.
[45] J. O. Krause, S. Lubbad, O. Nuyken, M. R. Buchmeiser, *Adv. Synth. Catal.* **2003**, *345*, 996–1004.
[46] J. O. Krause, O. Nuyken, K. Wurst, M. R. Buchmeiser, *Chem. Eur. J.* **2004**, *10*, 777–784.
[47] M. Mayr, B. Mayr, M. R. Buchmeiser, *Angew. Chem.* **2001**, *113*, 3957–3960; *Angew. Chem. Int. Ed.* **2001**, *40*, 3839–3842.
[48] P. Nieczypor, W. Buchowicz, W. J. N. Meester, F. Rutjes, J. C. Mol, *Tetrahedron Lett.* **2001**, *42*, 7103–7105.
[49] K. Vehlow, S. Maechling, K. Kohler, S. Blechert, *J. Organomet. Chem.* **2006**, *691*, 5267–5277.
[50] M. Ahmed, T. Arnauld, A. G. M. Barrett, D. C. Braddock, P. A. Procopiou, *Synlett* **2000**, 1007–1009.
[51] M. Ahmed, A. G. M. Barrett, D. C. Braddock, S. M. Cramp, P. A. Procopiou, *Tetrahedron Lett.* **1999**, *40*, 8657–8662.
[52] X. Elias, R. Pleixats, M. Wong Chi Man, *Tetrahedron* **2008**, *64*, 6770–6781.
[53] X. Elias, R. Pleixats, M. Wong Chi Man, J. J. E. Moreau, *Adv. Synth. Catal.* **2006**, *348*, 751–762.
[54] X. Elias, R. Pleixats, M. Wong Chi Man, J. J. E. Moreau, *Adv. Synth. Catal.* **2007**, *349*, 1701–1713.
[55] M. Samantaray, J. Alauzun, D. Gajan, S. Kavitake, A. Mehdi, L. Veyre, M. Lelli, A. Lesage, L. Emsley, C. Copéret, C. Thieuleux, *J. Am. Chem. Soc.* **2013**, *135*, 3193–3199.
[56] K. Melis, D. De Vos, P. Jacobs, F. Verpoort, *J. Mol. Catal. A* **2001**, *169*, 47–56.
[57] A. Monge-Marcet, R. Pleixats, X. Cattoen, M. Wong Chi Man, *J. Mol. Catal. A* **2012**, *357*, 59–66.
[58] A. Monge-Marcet, R. Pleixats, X. Cattoen, M. Wong Chi Man, *Tetrahedron* **2013**, *69*, 341–348.
[59] D. P. Allen, M. M. Van Wingerden, R. H. Grubbs, *Org. Lett.* **2009**, *11*, 1261–1264.
[60] I. Karamé, M. Boualleg, J. M. Camus, T. K. Maishal, J. Alauzun, J. M. Basset, C. Copéret, R. J. P. Corriu, E. Jeanneau, A. Mehdi, C. Reye, L. Veyre, C. Thieuleux, *Chem. Eur. J.* **2009**, *15*, 11820–11823.
[61] J. S. Kingsbury, A. H. Hoveyda, *J. Am. Chem. Soc.* **2005**, *127*, 4510–4517.
[62] K. Grela, M. Kim, *Eur. J. Org. Chem.* **2003**, 963–966.
[63] A. Michrowska, L. Gulajski, K. Grela, *Chem. Commun.* **2006**, 841–843.
[64] T. Vorfalt, K. J. Wannowius, V. Thiel, H. Plenio, *Chem. Eur. J.* **2010**, *16*, 12312–12315.
[65] L. Cavallo, *J. Am. Chem. Soc.* **2002**, *124*, 8965–8973.
[66] C. Costabile, L. Cavallo, *J. Am. Chem. Soc.* **2004**, *126*, 9592–9600.
[67] A. Poater, F. Ragone, A. Correa, L. Cavallo, *J. Am. Chem. Soc.* **2009**, *131*, 9000–9006.
[68] H. Clavier, A. Correa, E. C. Escudero-Adan, J. Benet-Buchholz, L. Cavallo, S. P. Nolan, *Chem. Eur. J.* **2009**, *15*, 10244–10254.
[69] F. Ragone, A. Poater, L. Cavallo, *J. Am. Chem. Soc.* **2010**, *132*, 4249–4258.
[70] Y. Zhao, D. G. Truhlar, *Org. Lett.* **2007**, *9*, 1967–1970.
[71] D. Benitez, E. Tkatchouk, W. A. Goddard, III, *Chem. Commun.* **2008**, 6194–6196.
[72] I. C. Stewart, D. Benitez, D. J. O'Leary, E. Tkatchouk, M. W. Day, W. A. Goddard, R. H. Grubbs, *J. Am. Chem. Soc.* **2009**, *131*, 1931–1938.
[73] P. Liu, X. Xu, X. Dong, B. K. Keitz, M. B. Herbert, R. H. Grubbs, K. N. Houk, *J. Am. Chem. Soc.* **2012**, *134*, 1464–1467.
[74] B. F. Straub, *Angew. Chem.* **2005**, *117*, 6129–6132; *Angew. Chem. Int. Ed.* **2005**, *44*, 5974–5978.
[75] C. Adlhart, P. Chen, *Angew. Chem.* **2002**, *114*, 4668–4671; *Angew. Chem. Int. Ed.* **2002**, *41*, 4484–4487.
[76] C. Adlhart, P. Chen, *J. Am. Chem. Soc.* **2004**, *126*, 3496–3510.
[77] G. Occhipinti, H. R. Bjorsvik, V. R. Jensen, *J. Am. Chem. Soc.* **2006**, *128*, 6952–6964.
[78] Y. Minenkov, G. Occhipinti, V. R. Jensen, *J. Phys. Chem. A* **2009**, *113*, 11833–11844.
[79] I. W. Ashworth, I. H. Hillier, D. J. Nelson, J. M. Percy, M. A. Vincent, *Chem. Commun.* **2011**, *47*, 5428–5430.
[80] P. van der Gryp, S. Marx, H. C. M. Vosloo, *J. Mol. Catal. A* **2012**, *355*, 85–95.
[81] F. Nuñez-Zarur, X. Solans-Monfort, L. Rodriguez-Santiago, R. Pleixats, M. Sodupe, *Chem. Eur. J.* **2011**, *17*, 7506–7520.
[82] F. Nuñez-Zarur, X. Solans-Monfort, L. Rodriguez-Santiago, M. Sodupe, *Organometallics* **2012**, *31*, 4203–4215.
[83] F. Nuñez-Zarur, X. Solans-Monfort, L. Rodriguez-Santiago, M. Sodupe, *ACS Catal.* **2013**, *3*, 206–218.
[84] X. Solans-Monfort, R. Pleixats, M. Sodupe, *Chem. Eur. J.* **2010**, *16*, 7331–7343.
[85] X. Solans-Monfort, E. Clot, C. Copéret, O. Eisenstein, *J. Am. Chem. Soc.* **2005**, *127*, 14015–14025.
[86] A. Poater, X. Solans-Monfort, E. Clot, C. Copéret, O. Eisenstein, *J. Am. Chem. Soc.* **2007**, *129*, 8207–8216.
[87] X. Solans-Monfort, C. Copéret, O. Eisenstein, *J. Am. Chem. Soc.* **2010**, *132*, 7750–7757.
[88] X. Solans-Monfort, C. Copéret, O. Eisenstein, *Organometallics* **2012**, *31*, 6812–6822.
[89] F. Nuñez-Zarur, J. Poater, L. Rodriguez-Santiago, X. Solans-Monfort, M. Sola, M. Sodupe, *Comput. Theor. Chem.* **2012**, *996*, 57–67.
[90] A. D. Becke, *J. Chem. Phys.* **1993**, *98*, 5648–5652.
[91] C. T. Lee, W. T. Yang, R. G. Parr, *Phys. Rev. B* **1988**, *37*, 785–789.
[92] W. J. Hehre, R. Ditchfield, J. A. Pople, *J. Chem. Phys.* **1972**, *56*, 2257–2261.
[93] M. M. Francl, W. J. Pietro, W. J. Hehre, J. S. Binkley, M. S. Gordon, D. J. Defrees, J. A. Pople, *J. Chem. Phys.* **1982**, *77*, 3654–3665.
[94] W. Küchle, M. Dolg, H. Stoll, H. Preuss, *Mol. Phys.* **1991**, *74*, 1245–1263.
[95] A. Bergner, M. Dolg, W. Kuchle, H. Stoll, H. Preuss, *Mol. Phys.* **1993**, *80*, 1431–1441.
[96] A. W. Ehlers, M. Bohme, S. Dapprich, A. Gobbi, A. Hollwarth, V. Jonas, K. F. Kohler, R. Stegmann, A. Veldkamp, G. Frenking, *Chem. Phys. Lett.* **1993**, *208*, 111–114.
[97] P. C. Hariharan, J. A. Pople, *Theor. Chim. Acta* **1973**, *28*, 213–222.
[98] M. Cossi, N. Rega, G. Scalmani, V. Barone, *J. Comput. Chem.* **2003**, *24*, 669–681.
[99] V. Barone, M. Cossi, J. Tomasi, *J. Chem. Phys.* **1997**, *107*, 3210–3221.
[100] P. Śliwa, J. Handzlik, *Chem. Phys. Lett.* **2010**, *493*, 273–278.
[101] S. Grimme, *J. Comput. Chem.* **2004**, *25*, 1463–1473.
[102] S. Grimme, *J. Comput. Chem.* **2006**, *27*, 1787–1799.
[103] P. Ugliengo, D. Viterbo, G. Chiari, *Z. Kristallogr.* **1993**, *207*, 9.
[104] M. J. Frisch, G. W. Trucks, H. B. Schlegel, G. E. Scuseria, M. A. Robb, J. R. Cheeseman, J. A. Montgomery Jr., T. Vreven,, K. N. Kudin, J. C. Burant, J. M. Millam, S. S. Iyengar, J. Tomasi, V. Barone, B. Mennucci, M. Cossi, G. Scalmani, N. Rega, G. A. Petersson, H. Nakatsuji, M. Hada, M. Ehara, K. Toyota, R. Fukuda, J. Hasegawa, M. Ishida, T. Nakajima, Y. Honda, O. Kitao, H. Nakai, M. Klene, X. Li, J. E. Knox, H. P. Hratchian, J. B. Cross, C. Adamo, J. Jaramillo, R. Gomperts, R. E. Stratmann, O. Yazyev, A. J. Austin, R. Cammi, C. Pomelli, J. W. Ochterski, P. Y. Ayala, K. Morokuma, G. A. Voth, P. Salvador, J. J. Dannenberg, V. G. Zakrzewski, S. Dapprich, A. D. Daniels, M. C. Strain, O. Farkas, D. K. Malick, A. D. Rabuck, K. Raghavachari, J. B. Foresman, J. V. Ortiz, Q. Cui, A. G. Baboul, S. Clifford, J. Cioslowski, B. B. Stefanov, G. Liu, A. Liashenko, P. Piskorz, I. Komaromi, R. L. Martin, D. J. Fox, T. Keith, M. A. Al-Laham, C. Y. Peng, A. Nanayakkara, M. Challacombe, P. M. W. Gill, B. Johnson, W. Chen, M. W. Wong, C. Gonzalez, J. A. Pople, Rev. B.04 ed., Gaussian Inc., Pittsburgh PA, **2003**.

[105] S. Sakaki, T. Takayama, M. Sumimoto, M. Sugimoto, *J. Am. Chem. Soc.* **2004**, *126*, 3332–3348.
[106] J. Cooper, T. Ziegler, *Inorg. Chem.* **2002**, *41*, 6614–6622.
[107] H. Jacobsen, L. Cavallo, *ChemPhysChem* **2012**, *13*, 1405–1406.
[108] H. Jacobsen, L. Cavallo, *ChemPhysChem* **2012**, *13*, 562–569.
[109] S. Grimme, *ChemPhysChem* **2012**, *13*, 1407–1409.
[110] A. G. D. Grotevendt, J. A. M. Lummiss, M. L. Mastronardi, D. E. Fogg, *J. Am. Chem. Soc.* **2011**, *133*, 15918–15921.
[111] G. C. Lloyd-Jones, R. G. Margue, J. G. de Vries, *Angew. Chem.* **2005**, *117*, 7608–7613; *Angew. Chem. Int. Ed.* **2005**, *44*, 7442–7447.
[112] T. Kitamura, Y. Sato, M. Mori, *Adv. Synth. Catal.* **2002**, *344*, 678–693.
[113] H. Villar, M. Frings, C. Bolm, *Chem. Soc. Rev.* **2007**, *36*, 55–66.
[114] V. Sashuk, K. Grela, *J. Mol. Catal. A* **2006**, *257*, 59–66.
[115] T. Vorfalt, K. J. Wannowius, H. Plenio, *Angew. Chem.* **2010**, *122*, 5665–5668; *Angew. Chem. Int. Ed.* **2010**, *49*, 5533–5536.
[116] V. Thiel, M. Hendann, K. J. Wannowius, H. Plenio, *J. Am. Chem. Soc.* **2012**, *134*, 1104–1114.
[117] G. C. Vougioukalakis, R. H. Grubbs, *Chem. Eur. J.* **2008**, *14*, 7545–7556.
[118] J. L. Hérisson, Y. Chauvin, *Makromol. Chem.* **1971**, *141*, 161.
[119] Y. Chauvin, *Angew. Chem.* **2006**, *118*, 3824–3831; *Angew. Chem. Int. Ed.* **2006**, *45*, 3740–3747.
[120] A. G. Wenzel, G. Blake, D. G. VanderVelde, R. H. Grubbs, *J. Am. Chem. Soc.* **2011**, *133*, 6429–6439.
[121] E. F. van der Eide, W. E. Piers, *Nat. Chem.* **2010**, *2*, 571–576.
[122] We have obtained the kinetic constants from our computed $G+\Delta G_{solv}+D$ energy barriers and using Eyring's equation. Afterwards the COPASI 4.8 package was used to numerically solve the differential equation.

Received: May 16, 2013
Published online: September 20, 2013

